ACS OMEGA

http://pubs.acs.org/journal/acsodf

Article

Development of a Redox-Label-Doped Molecularly Imprinted Polymer on β-Cyclodextrin/Reduced Graphene Oxide for Electrochemical Detection of a Stress Biomarker

Arpit Goyal and Toshiya Sakata*

Cite This: ACS Omega 2022, 7, 33491−33499

Read Online

ACCESS | Metrics & More | Article Recommendations | Supporting Information

ABSTRACT: Cortisol is a major stress biomarker involved in the regulation of metabolic and immune responses. Readily accessible assays with sufficient quantitative and temporal resolution can assist in prevention, early diagnosis, and management of chronic diseases. Whereas conventional assays are costly in terms of time, labor, and capital, an electrochemical approach offers the possibility of miniaturization and detection at the point-of-care. Here, we investigate the biosensor application of molecularly imprinted polypyrrole (PPy) doped with hexacyanoferrate (HCF) and coupled to reduced graphene oxide functionalized with β-cyclodextrin (β-CD). β-CD provides an inclusion site for lipophilic cortisol and was electrochemically grafted simultaneous with reduction of GO. Next, PPy was electrochemically deposited in presence of cortisol template with HCF dopant ions serving as intrinsic redox probe. Thus, the sensor response was evaluated via changes of redox peak current in cyclic voltammetry and demonstrated a broad logarithmic detection range (5 pg/mL to 5000 ng/mL, R^2 = 0.995), with a sensitivity of 8.809 μA $\log^{-1}$ (ng/mL) cm^{-2} and LOD of 19.3 pM. The sensor was shown to be specific toward cortisol in reference to salivary cortisol concentration in saliva over structural analogues. The sensor was exhibited to determine cortisol in artificial saliva at normal and elevated levels. The good performance and facile electrochemical fabrication of this antibody- and external label-free interface are promising for the development of affordable point-of-care biosensors.

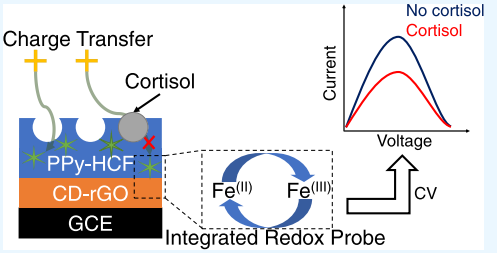

1. INTRODUCTION

Cortisol is a glucocorticoid hormone released by the adrenal glands in response to stress, either physiological or psychological, and it plays an essential role in stress management by regulating metabolism, glucose levels, cardiovascular systems, and immune responses.[1] Chronic stress can disrupt the normal levels of cortisol which can lead to illnesses such as diabetes, cardiovascular disease, depression, and Cushing's disease. Thus, detecting cortisol levels can assist in early disease diagnosis and timing of medical interventions.

Cortisol in blood serum is typically bound to proteins.[2] In other biological fluids (typically saliva, sweat, and urine), while cortisol is present, allowing for a noninvasive diagnostic option,[3,4] the concentrations are typically in the range of a few nM for healthy individuals (3.5−27 nM in saliva and 11−281 nM in urine[5]) and a broader range in the case of Cushing's patients (2.7−166 nM in saliva[6]). Thus, assays with sufficient sensitivity and specificity conventionally require chromatographic techniques or immunoassays (enzyme-linked immunosorbent assay), but they require laboratories with trained personnel.[7] Accordingly, such techniques require high costs in terms of time, labor, and capital, rendering them ill-suited for deployment as point-of-care (PoC) devices. To enable personalized healthcare, electrochemical biosensors are actively investigated as they can be fabricated affordably and the instrumentation can be miniaturized,[8] which makes it attractive for implementation in PoC devices. With the advancements in internet-of-things, mobile computing and networking technologies, electrochemical biosensors can be integrated with these technologies to enable a new generation of data-driven intelligent sensors for stress-free personal healthcare management.[9]

Early attempts at electrochemical cortisol detection involved adapting the immunometric methods from the lab onto the electrochemical transducers.[10] While antibodies exhibit high sensor performance, they are costly to isolate and prone to denaturation. An alternative to using natural receptors is to fabricate a molecularly imprinted polymer (MIP) containing target-specific sites that can selectively bind to the target molecule.[11] MIPs have several advantages over biological recognition elements such as ease of fabrication, stability, and affordability.[12] Recently, there has been some interest in designing and developing electrochemical sensors for cortisol

Received: July 13, 2022
Accepted: August 26, 2022
Published: September 7, 2022

by the bulk polymerization of MIPs using polymers methacrylic acid[13] and ethylene glycol.[14] In contrast, electrochemical polymerization techniques offer a simple, one-step process of directly depositing an MIP on the electrode surface with a greater degree of control over polymer morphology.[15] Computational studies have suggested that pyrrole-based polymers are suitable for fabricating cortisol-specific electrochemical MIP sensors.[16,17] The oxygen-containing electronegative functional groups present on the cortisol can interact with electropositive hydrogen attached to the nitrogen of pyrrole via hydrogen bonding, which helps in encapsulating cortisol in the polypyrrole (PPy) network during electropolymerization. Pyrrole can be electrochemically polymerized under ambient conditions, and the resulting PPy is stable and conductive in neutral pH, making it an excellent candidate for physiological MIPs and other sensing applications.[18,19]

Cyclodextrins (CDs) are a class of cyclic oligosaccharides of α-D-glucopyranose subunits, with β-CD consisting of seven such subunits. They are shaped as a frustum with amphiphilic properties—hydrophobic inner cavity and hydrophilic outer side. This allows β-CD to form supramolecular inclusion complexes with molecules of appropriate size; therefore, they are studied extensively for drug delivery.[20,21] The host−guest interactions between CDs and target molecules can be leveraged as a recognition signal, and indeed, CDs have been used in fabrication of sensors.[22−24] Because of this property, β-CD was selected to enhance the performance of the sensor. The combination of β-CD functioning as complimentary recognition sites in conjunction with MIP, which increases the template imprinting during MIP fabrication.[25] Graphene and its derivatives have been extensively studied for electrochemical biosensing applications,[26] in conjunction with antibodies as immunosensors[27,28] and aptamers.[29] Graphene oxide (GO) is an attractive interface material[30] which can be produced inexpensively by wet oxidation and exfoliation of graphite in comparison to traditional electrochemical electrodes. GO also provides high density of functional groups suitable for functionalization. GO can be electrochemically reduced to yield reduced GO (rGO), which offers high conductivity and while retaining the surface for functionalization. This allows for effective deposition of β-CD on the electrode surface.[31] Moreover, these properties of GO and rGO have been used in combination with MIPs to enhance their performance.[32] Hence, we have selected rGO as the base transducer in our study. A key challenge in deploying a sensor outside of a laboratory as a PoC device is scaling the manufacturing of the biosensor and related instrumentation. Inkjet and 3D printing are some of the most cost-effective and versatile methods of manufacturing, and these techniques can be utilized to produce GO-based printed electrodes at scale.[33,34]

Since cortisol and PPy are electrochemically stable, their interaction does not produce a redox signal and thus necessitates the use of an external redox label such as hexacyanoferrate (HCF) ($[Fe(CN)_6]^{3-/4-}$), which makes it difficult to develop it further as a miniature device. Internalization of such redox probes can be achieved by forming a charge complex during oxidation of pyrrole to PPy, which eliminates the need of an external label, simplifying the PoC application of the sensor. The PPy−HCF system has been investigated for biosensors and energy storage applications.[35−39]

In this investigation, to the best of the authors' knowledge, the present study is the first description of a cortisol sensor composed of a β-CD-functionalized rGO decorated with a cortisol-specific PPy MIP doped with HCF internal redox probe for the electrochemical determination of cortisol in physiological samples. CD was deposited on GO with its simultaneous reduction by cyclic voltammetry (CV). Imprinted PPy was utilized in conjunction with doped HCF, which offered external label-free signal, which was suppressed as target molecules bound to imprinted sites. The prepared sensor was shown to demonstrate sensitivity toward cortisol in a broad logarithmic range. The sensor was verified for determination of cortisol concentration in artificial saliva in reference ranges for both healthy and unhealthy salivary cortisol, thus exhibiting potential for implementation in noninvasive PoC cortisol diagnostic application.

2. MATERIALS AND METHODS

2.1. Materials. Cortisol ($C_{21}H_{30}O_5$, hydrocortisone), β-CD [$(C_6H_{10}O_5)_7$], potassium HCF(II) trihydrate ($K_4[Fe(CN)_6]\cdot 3H_2O$), potassium HCF(III) ($K_4[Fe(CN)_6]$), graphite powder, sulfuric acid (H_2SO_4, 98%), sodium nitrate ($NaNO_3$), potassium permanganate ($KMnO_4$), hydrogen peroxide (H_2O_2, 30% in water), 1 M hydrochloric acid (HCl), ethanol, dimethyl sulfoxide (DMSO), glucose, urea, sodium L-lactate, cholesterol, progesterone, testosterone, sodium chloride (NaCl), disodium hydrogen phosphate (Na_2HPO_4), anhydrous calcium chloride ($CaCl_2$), and mucin were procured from Fujifilm WAKO (Japan). Phosphate buffer saline (PBS, pH 7.4) and ultrapure water were obtained from Gibco (Thermofischer). Pyrrole (C_4H_5N) was obtained from Tokyo Chemicals (TCI, Japan). All chemicals were used as received. Rod-type glassy carbon electrodes (GCE, surface area = 0.07 cm^2) were obtained from ALS Co., Ltd. (Japan).

2.2. Material Characterization. Electrochemical syntheses and analyses were performed using an electrochemical analyzer (ALS/CH, model 618E) in a single-cell (glass vial, 23 mL, ALS), three-electrode setup which consisted of a (modified) GCE as the working electrode (WE), a platinum wire counter electrode (CE), and AglAgCll 3.3 M KCl reference electrode. Electrochemical characterization was performed by CV and electrochemical impedance spectroscopy (EIS) in PBS containing a 5 mM HCF redox probe. EIS was measured at a constant DC potential of 0.25 V with the amplitude of the sinusoidal AC potential set to 5 mV. The AC frequency was varied from 100 kHz to 0.1 kHz, and 12 data points per decade of frequency were collected. Scanning electron microscopy (SEM) was performed using an SM-200 SEM system (Topcon, Japan) with acceleration voltages of 5−15 kV.

2.3. Preparation of MIP Biosensor. GO was prepared from graphite powder using a modified Hummers' method.[30] GCE was polished using 0.05 μm alumina and then ultrasonicated in water, followed by ethanol, and then finally again in water. The GCE was then electrochemically cleaned in 0.5 M H_2SO_4 by CV for 10 cycles in the potential window of −1.0 to +1.0 V at a scan rate of 100 mV/s. After rinsing and drying the GCE, a 10 μL aliquot of 0.1 mg/mL GO suspension, which was homogenized by ultrasonication for 2 h, was drop-casted on the GCE surface and dried in ambient conditions to obtain GO/GCE. β-CD was electropolymerized on the GO/GCE surface by CV with PBS as the supporting electrolyte containing 0.01 M β-CD as the monomer. With

https://doi.org/10.1021/acsomega.2c04423
ACS Omega 2022, 7, 33491−33499

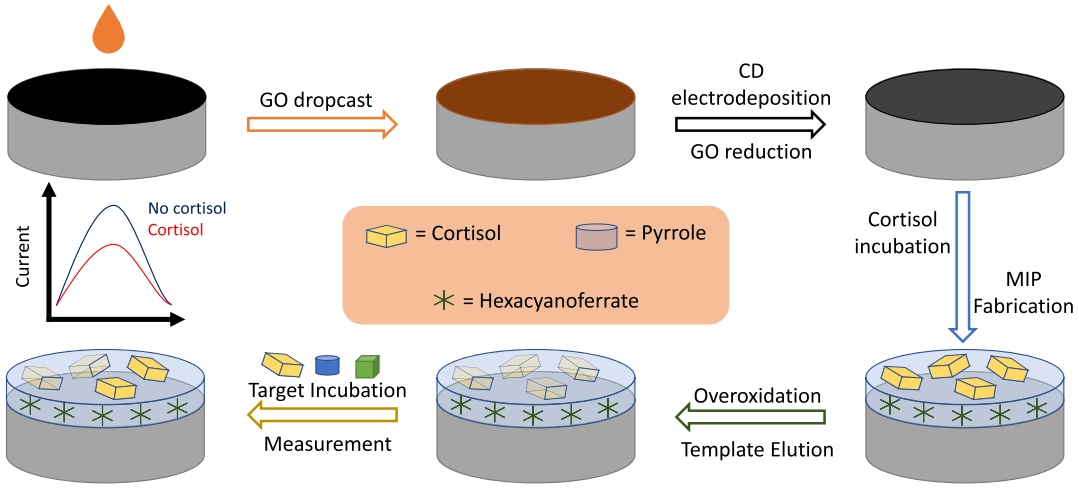

Figure 1. Schematic of Cortisol MIP sensor fabrication based on electropolymerization of pyrrole on CD−rGO/GCE doped with Cortisol and HCF.

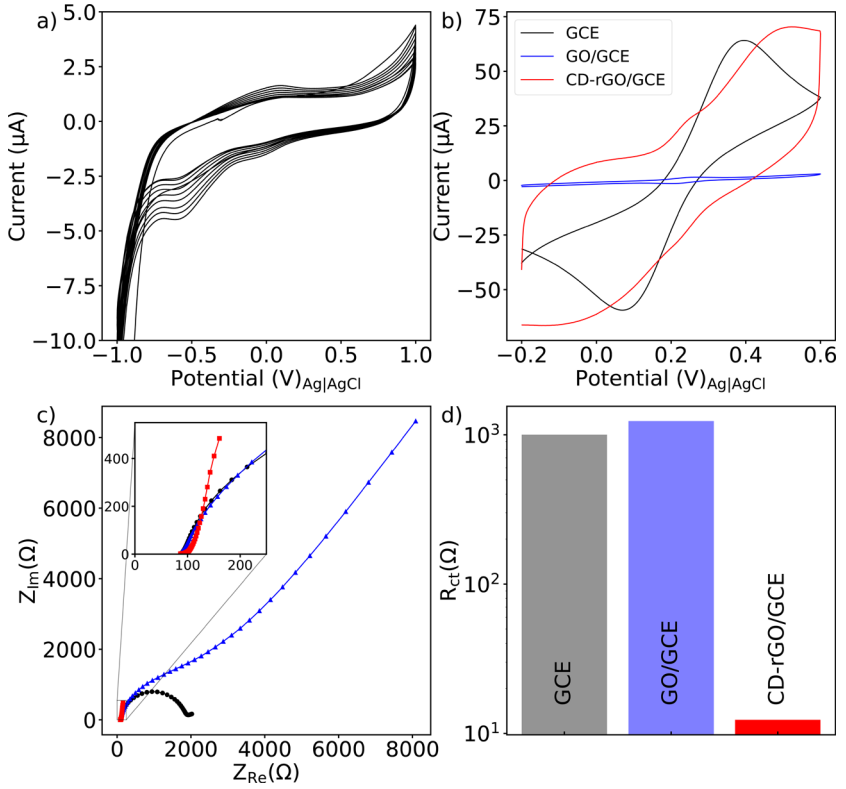

Figure 2. (a) CV response during electrochemical deposition of β-CD on GO/GCE. Electrochemical characterization of (modified) GCE during each stage of fabrication of CD−rGO/GCE in a 5 mM $[Fe(CN)_6]^{3-/4-}$ redox probe in PBS (pH 7.4) using (b) CV and (c) EIS. (d) R_{ct} values obtained during each modification.

GO/GCE as the WE, the potential was cycled continuously between −1.0 and 1.0 V at a scan rate of 20 mV/s for 10 cycles.[31] The resulting CD−rGO/GCE was washed gently with water and dried in air for later use.

Before proceeding with MIP fabrication, 10 mM cortisol (solubilized with help of DMSO) solution was prepared in PBS, and inclusion in CD−rGO/GCE was performed by immersion for 30 min. For MIP fabrication, an electropolymerization mixture was prepared using 5 mM cortisol, 5 mM $K_4[Fe(CN)_6]$, 5 mM $K_3[Fe(CN)_6]$, and 20 mM pyrrole in PBS. Nitrogen gas was bubbled through the mixture for 10 min to remove oxygen. Pyrrole was electropolymerized on the surface of CD−rGO/GCE by CV in the potential window of −0.2 to +0.9 V at a scan rate of 50 mV/s for 10 cycles to obtain PPy−CD−rGO/GCE.[15,17] After polymerization, the electrode was washed with PBS to remove unbound monomers. The template was eluted from the polymer matrix by overoxidation by CV in the potential window of −0.2 to +0.8 V in PBS containing 5 mM HCF at a scan rate of 50 mV/s for 20 cycles. The electrode was then washed with PBS and dried in nitrogen stream. The resulting electrode is hereafter referred to as the PPy−HCF/CD−rGO/GCE MIP. A non-

https://doi.org/10.1021/acsomega.2c04423
ACS Omega 2022, 7, 33491−33499

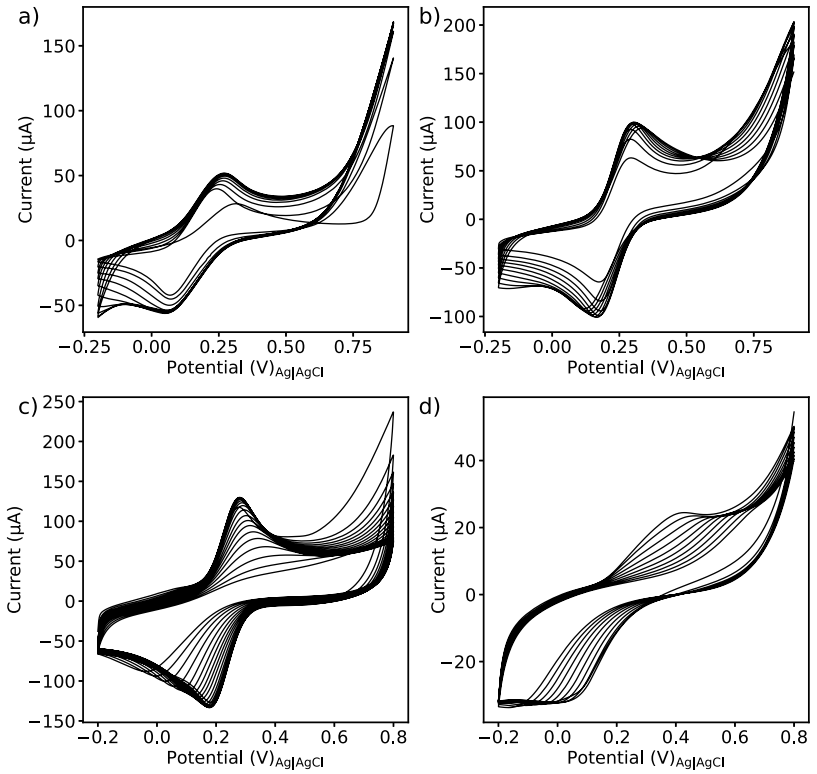

Figure 3. Cyclic voltammograms collected during (a) pyrrole electropolymerization with cortisol, (b) pyrrole electropolymerization without cortisol, (c) overoxidation of PPy−HCF to create MIP, and (d) overoxidation of PPy−HCF to create NIP.

imprinted polymer (NIP) version (PPy−HCF/CD−rGO/GCE NIP) of the MIP was prepared similarly, but without using cortisol in the fabrication process. The fabrication process is schematized in Figure 1.

2.4. Analytical Evaluation. The modified electrodes (MIP and NIP) were subjected to an electrochemical study using PBS as the electrolyte, which offer a standard and repeatable environment representative of a typical physiological pH, without any external redox probe. Calibration curve was obtained by recording the CV in the range of −0.5 to +0.5 V at 10 mV/s. Prior to the measurement, a 10 μL aliquot of the cortisol solution of predetermined concentration in PBS, prepared by diluting from a stock solution of 1 mg/mL cortisol in ethanol, was dropped on the electrode surface and allowed to incubate for 10 min. After measuring response at a given concentration, the sensors were gently washed with fresh PBS and response for the next aliquot was recorded.

To test the selectivity of the biosensor, signals obtained for 100 ng/mL interfering species were compared against signal obtained for 5 ng/mL cortisol, which represents the mean salivary cortisol concentration.[5] Glucose, lactate, cholesterol,[40] and urea[41] were used as they are common interfering species in saliva. Testosterone and progesterone were selected to represent the structural analogues of cortisol. A recovery study was performed using artificial saliva prepared from the procedure described by Usha et al.[42] Simply, 0.4 g/L of NaCl, 0.6 g/L of Na_2HPO_4, 4 g/L of urea, 0.6 g/L of $CaCl_2$, and 4 g/L of mucin were prepared in water and adjusted to a pH of 7.2. Artificial salivary cortisol samples were prepared by spiking cortisol to a known concentration. The samples were then diluted ten times in PBS prior to measurement.[6] Responses for artificial saliva samples were recorded using new sensors.

3. RESULTS AND DISCUSSION

3.1. Preparation of Cortisol Sensor. *3.1.1. Fabrication of CD−rGO/GCE.* Figure 2a shows the CV during fabrication of CD−rGO/GCE. The CV curve widened with each cycle, indicating an increase in conductivity due to reduction of GO to rGO with the simultaneous deposition of CD. A cathodic peak was observed at around −0.5 V, which is attributable to the reduction of oxygen-containing functional groups on GO and CD, whereas elevated currents near +1.0 V corresponding to the oxidation of the hydroxyl groups were observed on CD. During deposition, the primary hydroxyl groups present on CD undergo (partial) oxidation, which can form ester linkages with carboxylic acid groups present on GO.[43] In addition, a pair of weak peaks can be observed near 0 V and can be attributed to redox pairs of functional groups present on GO.[44]

Figure 2b shows the CV characterization of bare GCE, GO/GCE, and CD−rGO/GCE using 5 mM HCF redox probe in PBS. GCE showed characteristic redox peaks of HCF with peak currents of around 60 μA, whereas GO/GCE exhibited a suppressed voltammogram with small peaks of around 1.5 μA, indicating that GO inhibits the charge transfer from HCF to the electrode, which is possibly due to electrostatic repulsion of HCF by various oxygen-containing negatively charged functional groups on GO such as hydroxyl and carboxylic groups. This decreases the electrochemically active surface of GO for HCF, coupled with a decreased number of sp^2 carbon or graphitic characteristic, which affect the conductivity of the graphene material.[45] After the reduction of GO in the presence of CD, the currents increased markedly, slightly beyond those of bare GCE, implying the restoration of some graphitic characteristic.

These observations are corroborated by EIS measurements illustrated in Figure 2c in the presence of the HCF redox

https://doi.org/10.1021/acsomega.2c04423
ACS Omega 2022, 7, 33491−33499

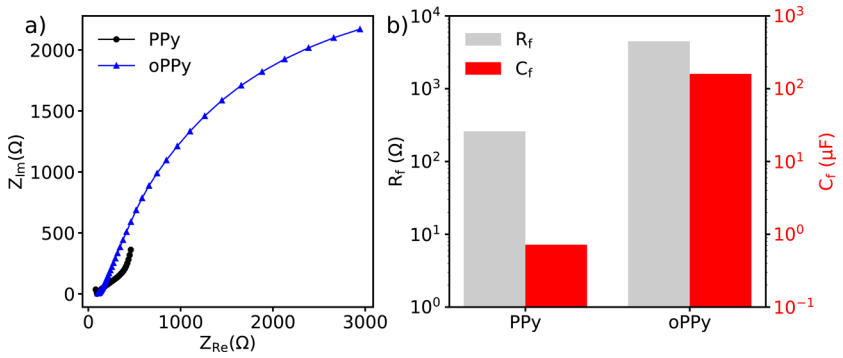

Figure 4. (a) EIS spectra of PPy (black) and overoxidized PPy (oPPy, blue). (b) Values of R_f (black, axis to the right) and C_f (red, axis to the left) extracted from the IES.

probe. The obtained spectra were fitted to Randle's equivalent circuit to characterize various sources of impedance. The circuit comprised charge-transfer resistance (R_{ct}) connected in series with diffusion or Warburg impedance (W), both of which were connected to double layer capacitance (C_{dl}) in parallel, and they were all finally connected in series with solution resistance (R_s). Although R_s is similar for (modified) GCEs (90 Ω), the rest of the spectra differs markedly, with main difference being the R_{ct}, which represents the charge transfer of the HCF redox probe at the electrode−electrolyte interface. As shown in Figure 2d, the values of R_{ct} for GCE and GO/GCE are similar, with that of GO/GCE being slightly larger (1234 Ω) than that of unmodified GCE (1002 Ω). However, after electrochemical modification of GO/GCE to CD−rGO/GCE, R_{ct} drops significantly (12.3 Ω). The errors are too small to be found on the graph (n = 3). This indicates that modification improves the charge transfer of HCF compared to bare GCE, which can serve as a basis for further modification with the MIP.

3.1.2. Fabrication of PPy−HCF MIP. Electrochemical methods enable PPy deposition on the electrode surface with ease and flexibility.[15] There are parameters such monomer and dopant concentration (see page S2 in Supporting Information) which can be adjusted to obtain polymer film suitable for the required application. In the case of MIP fabrication, the formation of a thick and dense polymer can lead to insufficient binding site formation and thus negatively affects the final sensitivity of the MIP. It can be controlled by adjusting monomer concentration. Monomer concentration is also determined by the concentration of template molecules. Since cortisol has limited solubility in aqueous media, it limits the amount of monomer that can be employed. For a noncovalent MIP, usually a monomer/template ratio of 4:1 is recommended for better stability of the monomer−template complex.[32,46]

Figure 3a shows the CV for PPy−HCF/CD−rGO/GCE MIP fabrication; the redox peaks associated with HCF are visible, with anodic and cathodic peaks settling at around 0.27 and 0.06 V, respectively, by the 10th cycle. The voltammogram widens with subsequent cycles, a characteristic indicating the formation of conducting polymers such as PPy,[15] although the separation becomes smaller, with a marginal difference by the 10th cycle, signifying the formation of a conductive PPy film of adequate thickness. Further cycling the potential leads to the formation of thicker PPy films, which can affect the sensitivity and performance of the resulting sensor. Hence, the number of electropolymerization cycles was fixed to 10. During electropolymerization, the cortisol template diffuses to the electrode surface and becomes incorporated into the PPy matrix. Comparing voltammograms collected during MIP versus NIP fabrication (Figure 3b), we observe higher currents for the NIP electropolymerization. Since cortisol is not an electrochemically active molecule, it hinders the charge transfer during MIP formation. In its absence, higher currents observed during NIP formation indicate the possibility of a thicker or denser PPy film.

After MIP electropolymerization, it is necessary to extract the embedded cortisol template and free up imprinted binding sites. This was achieved by overoxidation of PPy[47] which changes the charge density of the polymer and weakens hydrogen bonding between PPy and cortisol. The overoxidation method was adopted over elution using organic solvents so that the excess swelling or phase separation of PPy film can be avoided, which may distort the imprinted sites and negatively affect performance.[48] The overoxidation for elution was performed in PBS containing 5 mM HCF. The voltammogram for both the MIP and NIP (Figure 3c,d) is observed to be shrinking with successive cycles. In addition to template elution, overoxidation makes PPy dope with negatively charged hydroxyl and carbonyl groups,[15,47] which is observed as diminishing peaks of the HCF redox probe in Figure 3c. Concomitantly, the charge density on the PPy chain is altered and results in a partial dedoping of HCF counteranions from the PPy matrix as a new charge equilibrium is reached. As can be observed in Figure 3c,d, overoxidizing the MIP and NIP initiate an irreversible oxidation of the PPy−HCF matrix, with PPy getting doped with oxygen-containing groups and some HCF molecules ejected out as well.

The changes in the PPy film pre- and post-overoxidation were characterized by studying the EIS spectra extracted in the presence of the 5 mM HCF redox couple at 0.25 V and are presented in Figure 4a. Unlike Randle's circuit used to characterize the EIS spectra as in the case of the (modified) GCE electrodes in Section 3.1.1, a modified equivalent circuit diagram was fitted instead, which better describes the PPy behavior.[49] Here, the film resistance (R_f) and capacitance (C_f) are connected in parallel, with their combination connected serially with a constant phase element, which is assigned as a non-ideal double-layer capacitance. The overoxidation of PPy led to marked increases in both R_f (from 259 to 4485 Ω) and C_f (from 0.72 to 160 μF), which are shown in Figure 4b. The errors are too small to be found on the graph (n = 3).

3.2. SEM and EDS. SEM was conducted to observe the surface morphology after each step of modification during MIP

https://doi.org/10.1021/acsomega.2c04423
ACS Omega 2022, 7, 33491−33499

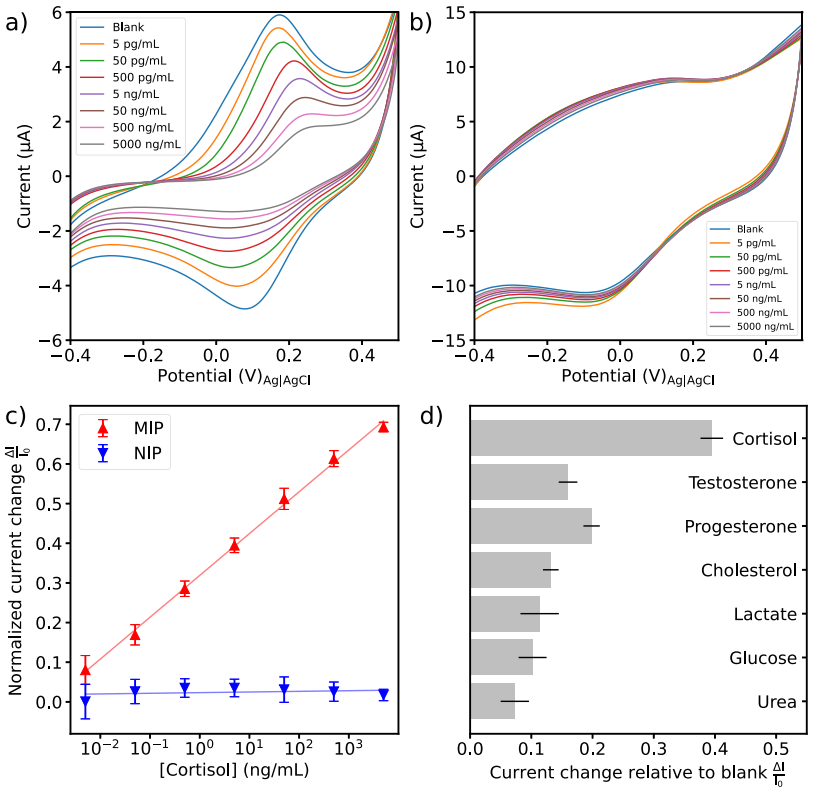

Figure 5. CV response collected in PBS with different cortisol concentration incubated (scan rate = 10 mV/s): (a) PPy−HCF/CD−rGO/GCE MIP and (b) PPy−HCF/CD−rGO/GCE NIP. (c) Calibration plot for relative current change versus cortisol concentration for MIP and NIP (n = 3). (d) Selectivity study using an MIP sensor response for 100 ng/mL interferents compared against 5 ng/mL cortisol. (n = 3).

fabrication. Figure S2a shows the drop-casted GO on the GCE. It can be observed that GO is deposited as thin layers with many folds, creases, and wrinkling on the surface along with some continuous areas. After the reduction of GO to rGO, the sp^2 characteristics of graphite starts to return, resulting in a higher planar structure. This planarity can be observed as a more rigid wrinkled morphology than in the case of GO in Figure S2b. The creases and folds have shrunk and become sharper in appearance. Figure S2c,d shows a SEM image of PPy. After electropolymerization, the surface is covered with micro-porous cauliflower-like structures, indicative of a networked structure of the PPy matrix.[15] The overoxidation of PPy leads to the dedoping of the PPy membrane, which elutes out the template as well as other ionic species. As a result, the cauliflower-like structures decrease in size, as seen in Figure S2e,f. Energy-dispersive X-ray spectroscopy (EDS) analysis was performed for the prepared MIP. The data are presented in Figure S3. Distinct peaks in the spectrum associated with iron confirms the presence of HCF in the prepared MIP.

3.3. Analytical Performance. The analytical performance of the sensor was evaluated by recording CV to different cortisol concentrations (Figure 5a) and characterizing the change in CV. Taking the anodic peak current around 0.2 V as a sensor response, we observe that increasing cortisol concentration for incubation decreases its magnitude. A broad range of cortisol concentrations was assessed, and it was found that the sensor response exhibited a linear relationship between the change in current from the baseline and the logarithmic change in cortisol concentration in the range of 5 pg/mL to 5000 ng/mL. Comparing the CV response of the MIP with the NIP in Figure 5b, the NIP shows a negligible change in current. This nonperformance of the NIP in capturing cortisol can be attributed to the absence of specific cortisol-binding sites. The imprinting process generates intrinsic sites suitable for and selective toward the target. Increasing the analyte concentration allows more target molecules to occupy those sites, thus increasing the impedance of the polymer for charge transfer, which manifests as a decrease in peak current in the voltammogram. Although PPy can still interact with cortisol via hydrogen bonding and contribute to the impedance, the lack of binding sites limits the adsorption of cortisol. In addition, voltammograms of NIP exhibited a slightly higher current than the MIP and the absence of a more pronounced anodic peak. A possible explanation for this is the formation of a denser PPy film during NIP electropolymerization.

Plotting the values of peak current obtained relative to the baseline (without any cortisol) against the cortisol concentration yields a calibration curve: $\Delta i(\mu A) = 0.6227 \times \log_{10}(c, \text{ng/mL}) + 1.8829$ in the range of 5 pg/mL to 5000 ng/mL in PBS with excellent linearity ($R^2 = 0.995$) and sensitivity (8.809 $\mu A\ \log^{-1}(\text{ng/mL})\ \text{cm}^{-2}$). The prepared MIP offered a broad range of cortisol concentrations with an LOD (3σ) of 19.3 pM for n = 3. The LOD is sufficiently low to noninvasively detect cortisol in various biological fluids such as sweat and saliva. In contrast, the slope of the NIP is nearly flat and may be attributed to the nonspecific interactions of cortisol with NIP (Figure 5c).

Comparison with other recent reports of cortisol sensors listed in Tables S1 and S2 suggests that the PPy−HCF/CD−rGO/GCE electrochemical MIP sensor prepared in this work offer broad logarithmic detection range and low LOD, which is sufficient for cortisol determination in biological samples such

https://doi.org/10.1021/acsomega.2c04423
ACS Omega 2022, 7, 33491−33499

as saliva and urine as well as diagnosing Cushing's disease. Unlike some MIPs which require external redox labels for detection, we have integrated HCF within the PPy matrix itself for external label-free cortisol detection, making it suitable for PoC application. The sensor discussed in this work is easy to fabricate as all the fabrication steps can be performed using electrochemical methods. Electrochemical sensing methods allow for PoC detection by miniaturizing the necessary instrumentation. In addition, the sensor is affordable to fabricate (cost analysis in Table S4) as the sensor does not employ expensive materials such as aptamers, antibodies, gold, and metalloporphyrin. The sensor is limited by the adsorption kinetics of MIP as evident by logarithmic sensitivity compared to linear sensitivity offered by some sensors reported in Tables S1 and S2. While the prepared sensor exhibits better sensitivity compared to other PPy based MIP,[17] it falls short compared to some reported cortisol immunosensor [72 μA $\log^{-1}$(g/mL)].[27] One of the future endeavors is to leverage computational tools which can help in characterization and optimization of materials and methods to enhance sensitivity and performance of the sensor.[9]

The response of the MIP can be fitted to an adsorption isotherm to understand the affinity of MIP toward the target.[50] Several common adsorption isotherm models including Langmuir, Freundlich, and Sips models[51,52] were considered. It was found that the Sips model (hybrid Langmuir–Freundlich model) offered the best fit

$$B = \frac{N_t a C^m}{1 + aC^m} \quad (1)$$

where B is related to the amount of the bound analyte, which in turn is related to the change in the peak current of signal after measurement. N_t is the representative binding site density. m is the heterogeneity index ranging from 0 to 1 (1 means completely homogeneous). a is related to affinity constant by $K_0 = a^{1/m}$. Fitting the curve to the Sips model yields m = 0.24, which indicates that the binding sites were highly heterogeneous in nature, which is a characteristic of a noncovalently formed MIP,[53] whereas the binding affinity was computed to be 1.6×10^7 M^{-1}, which is excellent for a noncovalent MIP when compared to binding affinities reported for other MIPs (Table S3).

3.4. Selectivity and Recovery. The relative change in signal obtained in the presence of 5 ng/mL cortisol were compared with response obtained for interfering species. The relative changes in the peak current of electrochemical signal are presented in Figure 5d. However, urea does not appreciably affect the signal response; comparatively, glucose and lactate produce slightly larger interference. Cortisol contains a lactate moiety that can allow lactate molecule to diffuse in the cavities. Glucose can react with other species during charge transfer, affecting the signals. Comparing with structural analogues, testosterone and progesterone hormones show greater changes in the MIP response. The hormones are structurally similar to cortisol since they are all derived from cholesterol, which can allow them to occupy the binding sites easily compared with other interferents. Cholesterol exhibited smaller response compared to the hormones which can be attributed to the large aliphatic branch on cholesterol hindering its interaction with the MIP. A normalized current change of 0.32 (on the X-axis of Figure 5d) correlates to the lower limit of reference salivary cortisol (3.5 nM), while the interferents exhibited significantly lesser normalized current change, which implies that the nonspecific response of the interferents do not meaningfully affect the sensor performance in the reference salivary cortisol concentration range.

Clinical applicability was investigated by spiking cortisol into artificial saliva at concentrations representative of healthy and unhealthy levels. The artificial samples were diluted 10× with PBS prior to the measurement. The measurements shown in Table 1 exhibit satisfactory recovery (96–109%) in the range of 1–500 ng/mL, which covers a broad range of salivary cortisol levels in healthy and unhealthy individuals. The future work will involve investigating the fabrication of miniature two-dimensional sensors based on materials and methods discussed in this study and employing them as a PoC device to determine cortisol levels in real clinical samples.

Table 1. Measurement of Cortisol in Artificial Saliva Samples (n = 3)

initial concentration (ng/mL)	concentration after dilution (ng/mL)	concentration measured (ng/mL)	recovery (%)
1	0.1	0.109 ± 0.019	109.31
2	0.2	0.193 ± 0.054	96.58
5	0.5	0.502 ± 0.071	100.41
10	1	1.04 ± 0.07	104.60
20	2	2.05 ± 0.12	102.67
50	5	5.25 ± 0.33	105.13
100	10	9.73 ± 0.58	97.28
200	20	19.9 ± 2.05	99.60
500	50	52.2 ± 0.58	104.47

4. CONCLUSIONS

A β-CD/rGO decorated with the HCF redox probe-doped PPy was successfully fabricated as a molecularly imprinted biosensor for cortisol. CD was electrochemically deposited on GO with concurrent reduction to rGO to prepare an inexpensive conductive electrode material. PPy MIP was electropolymerized on the CD–rGO/GCE surface using CV. The internalization of HCF redox probes enabled the detection of the changes in film impedance as a better readable redox signal strength. The prepared PPy–CD–rGO/GCE MIP exhibited a linear response with respect to logarithmic cortisol concentration in a broad range from 5 pg/mL to 5000 ng/mL with a low detection limit of 19.3 pM, which is satisfactory for determining cortisol in biological fluids. The biosensor also demonstrated specificity toward cortisol, not to various interferents. The methods and materials discussed in this study can be applied to the fabrication of similar biosensors for other stress biomarkers such as serotonin. Furthermore, the methods can be used to prepare a miniature sensing device based on field effect transistors..

■ ASSOCIATED CONTENT

Supporting Information

The Supporting Information is available free of charge at https://pubs.acs.org/doi/10.1021/acsomega.2c04423.

Effect on the PPy–HCF MIP sensor due to HCF and pyrrole monomer concentrations; SEM images of GO, rGO, and PPy pre- and post-oxidation; EDS analysis of PPy–HCF MIP; list of recent reports of cortisol MIP biosensors compared with this work; comparison of this work with other types of recently reported cortisol

https://doi.org/10.1021/acsomega.2c04423
ACS Omega 2022, 7, 33491–33499

biosensors, and list of MIPs with reported binding (or dissociation) constant (PDF)

AUTHOR INFORMATION

Corresponding Author

Toshiya Sakata − *Department of Materials Engineering, School of Engineering, The University of Tokyo, Bunkyo-ku, Tokyo 113-8656, Japan;* orcid.org/0000-0003-1246-5000; Phone: +81-3-5841-1842; Email: sakata@biofet.t.u-tokyo.ac.jp; Fax: +81-3-5841-1842

Author

Arpit Goyal − *Department of Materials Engineering, School of Engineering, The University of Tokyo, Bunkyo-ku, Tokyo 113-8656, Japan*

Complete contact information is available at: https://pubs.acs.org/10.1021/acsomega.2c04423

Notes

The authors declare no competing financial interest.

ACKNOWLEDGMENTS

This study was partly supported by the Program on Open Innovation Platform with Enterprises, Research Institute and Academia (OPERA) of Japan Science and Technology (JST).

REFERENCES

(1) Thau, L.; Gandhi, J.; Sharma, S. *StatPearls*; StatPearls Publishing: Treasure Island (FL), 2021.

(2) Lee, D. Y.; Kim, E.; Choi, M. H. Technical and clinical aspects of cortisol as a biochemical marker of chronic stress. *BMB Rep.* **2015**, *48*, 209−216.

(3) Hellhammer, D. H.; Wüst, S.; Kudielka, B. M. Salivary cortisol as a biomarker in stress research. *Psychoneuroendocrinology* **2009**, *34*, 163−171.

(4) Parlak, O. Portable and wearable real-time stress monitoring: A critical review. *Sensor. Actuator. Rep.* **2021**, *3*, 100036.

(5) Panahi, Z.; Ren, T.; Halpern, J. M. Nanostructured Cyclodextrin-Mediated Surface for Capacitive Determination of Cortisol in Multiple Biofluids. *ACS Appl. Mater. Interfaces* **2022**, DOI: 10.1021/acsami.2c07701.

(6) Yeasmin, S.; Wu, B.; Liu, Y.; Ullah, A.; Cheng, L.-J. Nano gold-doped molecularly imprinted electrochemical sensor for rapid and ultrasensitive cortisol detection. *Biosens. Bioelectron.* **2022**, *206*, 114142.

(7) Zea, M.; Bellagambi, F. G.; Ben Halima, H.; Zine, N.; Jaffrezic-Renault, N.; Villa, R.; Gabriel, G.; Errachid, A. Electrochemical sensors for cortisol detections: Almost there. *Trends Anal. Chem.* **2020**, *132*, 116058.

(8) Cruz, A. F. D.; Norena, N.; Kaushik, A.; Bhansali, S. A low-cost miniaturized potentiostat for point-of-care diagnosis. *Biosens. Bioelectron.* **2014**, *62*, 249−254.

(9) Chaudhary, V.; Kaushik, A.; Furukawa, H.; Khosla, A. Review—Towards 5th Generation AI and IoT Driven Sustainable Intelligent Sensors Based on 2D MXenes and Borophene. *ECS Sens. Plus* **2022**, *1*, 013601.

(10) Kaushik, A.; Vasudev, A.; Arya, S. K.; Pasha, S. K.; Bhansali, S. Recent advances in cortisol sensing technologies for point-of-care application. *Biosens. Bioelectron.* **2014**, *53*, 499−512.

(11) Sakata, T. Biologically Coupled Gate Field-Effect Transistors Meet in Vitro Diagnostics. *ACS Omega* **2019**, *4*, 11852−11862.

(12) Sakata, T.; Nishitani, S.; Kajisa, T. Molecularly imprinted polymer-based bioelectrical interfaces with intrinsic molecular charges. *RSC Adv.* **2020**, *10*, 16999−17013.

(13) Parlak, O.; Keene, S. T.; Marais, A.; Curto, V. F.; Salleo, A. Molecularly selective nanoporous membrane-based wearable organic electrochemical device for noninvasive cortisol sensing. *Sci. Adv.* **2018**, *4*, No. eaar2904.

(14) Mugo, S. M.; Alberkant, J. Flexible molecularly imprinted electrochemical sensor for cortisol monitoring in sweat. *Anal. Bioanal. Chem.* **2020**, *412*, 1825−1833.

(15) Manickam, P.; Pasha, S. K.; Snipes, S. A.; Bhansali, S. A Reusable Electrochemical Biosensor for Monitoring of Small Molecules (Cortisol) Using Molecularly Imprinted Polymers. *J. Electrochem. Soc.* **2016**, *164*, B54.

(16) Manickam, P.; Arizaleta, F.; Gurusamy, M.; Bhansali, S. Theoretical Studies of Cortisol-Imprinted Prepolymerization Mixtures: Structural Insights into Improving the Selectivity of Affinity Sensors. *J. Electrochem. Soc.* **2017**, *164*, B3077.

(17) Tang, W.; Yin, L.; Sempionatto, J. R.; Moon, J.-M.; Teymourian, H.; Wang, J. Touch-Based Stressless Cortisol Sensing. *Adv. Mater.* **2021**, *33*, No. e2008465.

(18) Palanisamy, S.; Thangavelu, K.; Chen, S.-M.; Velusamy, V.; Chang, M.-H.; Chen, T.-W.; Al-Hemaid, F. M. A.; Ali, M. A.; Ramaraj, S. K. Synthesis and characterization of polypyrrole decorated graphene/β-cyclodextrin composite for low level electrochemical detection of mercury (II) in water. *Sens. Actuators, B* **2017**, *243*, 888−894.

(19) Pour, B. H.; Haghnazari, N.; Keshavarzi, F.; Ahmadi, E.; Zarif, B. R. A sensitive sensor based on molecularly imprinted polypyrrole on reduced graphene oxide modified glassy carbon electrode for nevirapine analysis. *Anal. Methods* **2021**, *13*, 4767−4777.

(20) Fenyvesi, É.; Puskás, I.; Szente, L. Applications of steroid drugs entrapped in cyclodextrins. *Environ. Chem. Lett.* **2019**, *17*, 375−391.

(21) Dhiman, P.; Bhatia, M. Pharmaceutical applications of cyclodextrins and their derivatives. *J. Inclusion Phenom. Macrocyclic Chem.* **2020**, *98*, 171−186.

(22) Agnihotri, N.; Chowdhury, A. D.; De, A. Non-enzymatic electrochemical detection of cholesterol using β-cyclodextrin functionalized graphene. *Biosens. Bioelectron.* **2015**, *63*, 212−217.

(23) Suda, N.; Sunayama, H.; Kitayama, Y.; Kamon, Y.; Takeuchi, T. Oriented, molecularly imprinted cavities with dual binding sites for highly sensitive and selective recognition of cortisol. *R. Soc. Open Sci.* **2017**, *4*, 170300.

(24) Zhao, X.; Wang, Y.; Zhang, P.; Lu, Z.; Xiao, Y. Recent Advances of Molecularly Imprinted Polymers Based on Cyclodextrin. *Macromol. Rapid Commun.* **2021**, *42*, No. e2100004.

(25) Lu, B.; Xia, J.; Wang, Z.; Zhang, F.; Yang, M.; Li, Y.; Xia, Y. Molecularly imprinted electrochemical sensor based on an electrode modified with an imprinted pyrrole film immobilized on a β-cyclodextrin/gold nanoparticles/graphene layer. *RSC Adv.* **2015**, *5*, 82930−82935.

(26) Thangamuthu, M.; Hsieh, K. Y.; Kumar, P. V.; Chen, G.-Y. Graphene- and Graphene Oxide-Based Nanocomposite Platforms for Electrochemical Biosensing Applications. *Int. J. Mol. Sci.* **2019**, *20*, 2975.

(27) Nasyifa, M. M. N.; Ruslinda, A. R.; Halim, N. H. A.; Abidin, A. S. Z.; Faudzi, F. N. M.; Ahmad, N. A.; Lockman, Z.; Rezek, B.; Kromka, A.; Gopinath, S. C. B. Immuno-probed graphene nanoplatelets on electrolyte-gated field-effect transistor for stable cortisol quantification in serum. *J. Taiwan Inst. Chem. Eng.* **2020**, *117*, 10−18.

(28) Gwiazda, M.; Kaushik, A.; Chlanda, A.; Kijeńska-Gawrońska, E.; Jagiełło, J.; Kowiorski, K.; Lipińska, L.; Święszkowski, W.; Bhardwaj, S. K. A flexible immunosensor based on the electrochemically rGO with Au SAM using half-antibody for collagen type I sensing. *Appl. Surf. Sci. Adv.* **2022**, *9*, 100258.

(29) Abidin, A. S. Z.; Rahim, R. A.; Md Arshad, M. K.; Nabilah, M. F.; Voon, C. H.; Tang, T.-H.; Citartan, M. Current and Potential Developments of Cortisol Aptasensing towards Point-of-Care Diagnostics (POTC). *Sensors* **2017**, *17*, 1180.

(30) Bairagi, P. K.; Goyal, A.; Verma, N. Methyl nicotinate biomarker of tuberculosis voltammetrically detected on cobalt nanoparticle-dispersed reduced graphene oxide-based carbon film in blood. *Sens. Actuators, B* **2019**, *297*, 126754.

(31) Qin, Q.; Bai, X.; Hua, Z. Electropolymerization of a conductive β-cyclodextrin polymer on reduced graphene oxide modified screen-printed electrode for simultaneous determination of ascorbic acid, dopamine and uric acid. *J. Electroanal. Chem.* **2016**, *782*, 50−58.
(32) Singhal, A.; Sadique, M. A.; Kumar, N.; Yadav, S.; Ranjan, P.; Parihar, A.; Khan, R.; Kaushik, A. K. Multifunctional carbon nanomaterials decorated molecularly imprinted hybrid polymers for efficient electrochemical antibiotics sensing. *J. Environ. Chem. Eng.* **2022**, *10*, 107703.
(33) Porro, S.; Ricciardi, C. Memristive behaviour in inkjet printed graphene oxide thin layers. *RSC Adv.* **2015**, *5*, 68565−68570.
(34) Fu, K.; Wang, Y.; Yan, C.; Yao, Y.; Chen, Y.; Dai, J.; Lacey, S.; Wang, Y.; Wan, J.; Li, T.; Wang, Z.; Xu, Y.; Hu, L. Graphene Oxide-Based Electrode Inks for 3D-Printed Lithium-Ion Batteries. *Adv. Mater.* **2016**, *28*, 2587−2594.
(35) Fiorito, P. A.; de Torresi, S. I. C. Hybrid nickel hexacyanoferrate/polypyrrole composite as mediator for hydrogen peroxide detection and its application in oxidase-based biosensors. *J. Electroanal. Chem.* **2005**, *581*, 31−37.
(36) Fiorito, P. A.; Brett, C. M. A.; Cordobadetorresi, S. I. Polypyrrole/copper hexacyanoferrate hybrid as redox mediator for glucose biosensors. *Talanta* **2006**, *69*, 403−408.
(37) Duan, D.; Si, X.; Ding, Y.; Li, L.; Ma, G.; Zhang, L.; Jian, B. A novel molecularly imprinted electrochemical sensor based on double sensitization by MOF/CNTs and Prussian blue for detection of 17β-estradiol. *Bioelectrochemistry* **2019**, *129*, 211−217.
(38) Ensafi, A. A.; Ahmadi, N.; Rezaei, B. Electrochemical preparation and characterization of a polypyrrole/nickel-cobalt hexacyanoferrate nanocomposite for supercapacitor applications. *RSC Adv.* **2015**, *5*, 91448−91456.
(39) Lee, P. K.; Woi, P. M. Current Innovations of Metal Hexacyanoferrates-Based Nanocomposites toward Electrochemical Sensing: Materials Selection and Synthesis Methods. *Crit. Rev. Anal. Chem.* **2020**, *50*, 393−404.
(40) Ngamchuea, K.; Chaisiwamongkhol, K.; Batchelor-McAuley, C.; Compton, R. G. Chemical analysis in saliva and the search for salivary biomarkers - a tutorial review. *Analyst* **2017**, *143*, 81−99.
(41) Peng, C.-H.; Xia, Y.-C.; Wu, Y.; Zhou, Z.-F.; Cheng, P.; Xiao, P. Influencing factors for saliva urea and its application in chronic kidney disease. *Clin. Biochem.* **2013**, *46*, 275−277.
(42) Usha, S. P.; Shrivastav, A. M.; Gupta, B. D. A contemporary approach for design and characterization of fiber-optic-cortisol sensor tailoring LMR and ZnO/PPY molecularly imprinted film. *Biosens. Bioelectron.* **2017**, *87*, 178−186.
(43) Pereira, A. C.; Oliveira, A. E. F.; Bettio, G. B. β-Cyclodextrin electropolymerization: mechanism, electrochemical behavior, and optimization. *Chem. Pap.* **2019**, *73*, 1795−1804.
(44) Essousi, H.; Barhoumi, H.; Karastogianni, S.; Girousi, S. T. An electrochemical sensor based on reduced graphene oxide, gold nanoparticles and molecular imprinted over-oxidized polypyrrole for amoxicillin determination. *Electroanalysis* **2020**, *32*, 1546−1558.
(45) Singh, M.; Yadav, A.; Kumar, S.; Agarwal, P. Annealing induced electrical conduction and band gap variation in thermally reduced graphene oxide films with different sp2/sp3 fraction. *Appl. Surf. Sci.* **2015**, *326*, 236−242.
(46) Hasanah, A. N.; Safitri, N.; Zulfa, A.; Neli, N.; Rahayu, D. Factors Affecting Preparation of Molecularly Imprinted Polymer and Methods on Finding Template-Monomer Interaction as the Key of Selective Properties of the Materials. *Molecules* **2021**, *26*, 1.
(47) Shiigi, H.; Yakabe, H.; Kishimoto, M.; Kijima, D.; Zhang, Y.; Sree, U.; Deore, B. A.; Nagaoka, T. Molecularly Imprinted Overoxidized Polypyrrole Colloids: Promising Materials for Molecular Recognition. *Microchim. Acta* **2003**, *143*, 155−162.
(48) Gillan, L.; Jansson, E. Molecularly imprinted polymer on roll-to-roll printed electrodes as a single use sensor for monitoring of cortisol in sweat. *Flex. Print. Electron.* **2022**, *7*, 025014.
(49) Ramanavicius, A.; Finkelsteinas, A.; Cesiulis, H.; Ramanaviciene, A. Electrochemical impedance spectroscopy of polypyrrole based electrochemical immunosensor. *Bioelectrochemistry* **2010**, *79*, 11−16.
(50) Kajisa, T.; Li, W.; Michinobu, T.; Sakata, T. Well-designed dopamine-imprinted polymer interface for selective and quantitative dopamine detection among catecholamines using a potentiometric biosensor. *Biosens. Bioelectron.* **2018**, *117*, 810−817.
(51) Jin, Y.; Row, K. H. Adsorption isotherm of ibuprofen on molecular imprinted polymer. *Korean J. Chem. Eng.* **2005**, *22*, 264−267.
(52) Abu-Alsoud, G. F.; Hawboldt, K. A.; Bottaro, C. S. Comparison of Four Adsorption Isotherm Models for Characterizing Molecular Recognition of Individual Phenolic Compounds in Porous Tailor-Made Molecularly Imprinted Polymer Films. *ACS Appl. Mater. Interfaces* **2020**, *12*, 11998−12009.
(53) Umpleby, R. J., 2nd; Baxter, S. C.; Chen, Y.; Shah, R. N.; Shimizu, K. D. Characterization of molecularly imprinted polymers with the Langmuir-Freundlich isotherm. *Anal. Chem.* **2001**, *73*, 4584−4591.

https://doi.org/10.1021/acsomega.2c04423
ACS Omega 2022, 7, 33491−33499